

# The Synthesis and Characterization of Acrylic Polymer with 1,2,3-Benzotriazole Pendant Groups

ISSN: 2770-6613

**Mariano Galán<sup>1</sup>, Valeria Pozzoli<sup>2</sup> and Miriam Martins Alho<sup>3\*</sup>**

Universidad de Buenos Aires, Facultad de Ingeniería, Laboratorio de Materiales Orgánicos (LabMOR), Instituto de Química Aplicada a la Ingeniería (IQAI), Buenos Aires, Argentina

## Abstract

In order to perform future studies on the anticorrosive effect generated by the inclusion of benzotriazoles in anticorrosive mixtures, we performed the synthesis of a new polyacrylate containing benzotriazole as pendant groups. We have explored the reaction of 1,2,3-benzotriazole with ethanolamine and formaldehyde in a 2:1:2 ratio with the purpose of including an aliphatic spacer that reduces steric hindrance during polymerization. We have found that oxygen can also participate in the reaction as well as amine. We have synthesized the 2-(bis((1*H*-Benzo[*d*] [1,2,3] triazol-1-yl) Methylamino) Ethyl Acrylate (BMEA) monomer, which includes two pendant benzotriazole groups. After the synthesis of this monomer, we obtained the new material (PBMEA) by a solution polymerization. This material has a great trend to absorb moisture in contact with the air and we determine that this absorption seems stoichiometric.

**Keywords:** Polymer; Benzotriazole; Ethanolamine; Synthesis

**\*Corresponding author:** Miriam Martins Alho, Universidad de Buenos Aires, Facultad de Ingeniería, Laboratorio de Materiales Orgánicos (LabMOR), Instituto de Química Aplicada a la Ingeniería (IQAI), Buenos Aires, Argentina

**Submission:**  February 24, 2023**Published:**  April 21, 2023

Volume 4 - Issue 5

**How to cite this article:** Mariano Galán, Valeria Pozzoli and Miriam Martins Alho\*. The Synthesis and Characterization of Acrylic Polymer with 1,2,3-Benzotriazole Pendant Groups. *Polymer Sci peer Rev J.* 4(5). PSPRJ. 000600. 2023.  
DOI: [10.31031/PSPRJ.2023.04.000600](https://doi.org/10.31031/PSPRJ.2023.04.000600)

**Copyright@** Miriam Martins Alho, This article is distributed under the terms of the Creative Commons Attribution 4.0 International License, which permits unrestricted use and redistribution provided that the original author and source are credited.

## Introduction

Benzotriazole is a very versatile heterocycle, as well as synthetic auxiliary [1] or ligand in reactions like Heck, Sonogashira and Suzuki [2]. This heterocycle also has possibilities of binding to receptors and enzymes, exhibiting a wide range of biological activities, like plant growing regulator [3], antibacterial [4] and antiviral [5-8]. Benzotriazole is used in several industrial products, like UV stabilizer in plastics, waxes, and in dishwasher detergents as anticorrosive [9-12]. Benzotriazole is an effective surface anticorrosive agent, both on objects exposed to the air and on submerged materials, because it forms a multilayer covering by chemisorption with iron, that not only inhibits corrosion, but also improves coating adhesion [13]. As corrosion causes economic losses by millions annually, in the past years technologies based on Zr and/or Ti have emerged to replace the effective but dangerous Cr (VI) treatment [14,15]. These chromium-free anticorrosive mixtures include several types of polymers [16], which usually fulfill the role of making the treated surface more compatible with the anticorrosive coating and paint, offering an improved protection. Benzotriazole has been included in some of these mixtures as microcapsules or nanocontainers, acting in some cases as "self-repair" agents when the applied physical barriers fail [17-19]. Despite there are only a few records of the inclusion of benzotriazoles as part of the polymeric matrix [20], some results were promising. In this work we decided to explore the possibility to obtain a homopolymer containing benzotriazole as pendant groups of the main chain, in the aim of using it into anticorrosive mixtures. This material could give rise to new anticorrosive treatments with better adhesion and self-healing effect.

## Experimental

### General

Benzoyl Peroxide (BPO) were provided by Teyupa S.A. Acrylic acid, thionyl chloride and benzotriazole were purchased from Merck. Ethanolamine and formaldehyde were purchased to Anedra. Solvents were purchased from Sintorgan S.A. and distilled before used. <sup>1</sup>H and <sup>13</sup>C NMR

were recorded on a Bruker AMX-500 from Bruker Corporation (500 and 125MHz, respectively, Universidad de Buenos Aires, Facultad de Ciencias Exactas y Naturales, UMYMFOR), in CDCl<sub>3</sub> or DMSO-d<sub>6</sub>. IR spectra were performed on a Nicolet 6700 spectrometer from Thermo Scientific (Instituto Tecnológico de Buenos Aires) and TGA analysis was recorded on a TGA-50 Shimadzu Analyzer from Shimadzu Corporation (Universidad de Buenos Aires, Facultad de Ingeniería, ITPN) at 5 °C/min under nitrogen flow.

### Synthesis of 2-((1*H*-benzo[*d*] [1,2,3] triazol-1-yl) methylamino) ethanol (1)

In a round bottom flask, 1.19g (10mmol) were weighed and dissolved in 25mL of THF. Next, 0.61mL (10mmol) of ethanolamine was added and the mixture was allowed to stir for 5 minutes. Then, 0.84mL (10mmol) of 40% formaldehyde were added and the mixture was allowed to stir for 3h at room temperature. After that period, the solvent was evaporated, and the residue was dissolved in HCCl<sub>3</sub> (20mL). The organic layer was washed with distilled water (3x10mL), dried with Na<sub>2</sub>SO<sub>4</sub>, filtered, and evaporated. The residue was purified by flash chromatography and obtaining 1.3g of product, which is equivalent to a 68% of non-optimized yield.

### Synthesis of 2-(1*H*-bis((benzo[*d*] [1,2,3] triazol-1-yl) methylamino) ethanol (3)

In a round bottom flask, 1.19g (10mmol) of benzotriazole were suspended in 10mL of distilled water and then 0.3mL (5mmol) of ethanolamine obtaining a clear solution which was stirred for 10 minutes at room temperature. Then, 0.82mL of formaldehyde (40%, 10.1mmol) was added dropwise. After 2.5h, a rubbery solid appeared at the bottom. The aqueous medium was discarded, and the precipitate washed with distilled water (3 times, 20mL each), and dissolved in 20mL of acetone. The organic dissolution was dried with Na<sub>2</sub>SO<sub>4</sub>, filtered and the solvent eliminated using reduced pressure, obtaining title compound in a non-optimized yield of 76% (1.32g). Compound 3a: (<sup>1</sup>H NMR, δ) 7.99 (H-4), 7.73 (H-7), 7.45 (H-5), 7.33 (H-6), 5.69 (CH<sub>2</sub>-1'), 3.78 (CH<sub>2</sub>-2'), 3.12 (CH<sub>2</sub>-3'), 1.20 (-OH). (<sup>13</sup>C NMR, δ) 145.8 (C-3a), 133.2 (C-7a), 128.0 (C-6), 124.4 (C-5), 119.7 (C-4), 110.1 (C-7), 64.8 (C-1'), 60.6 (C-3') 53.3 (C-2'). Compound 3b: (<sup>1</sup>H NMR, δ N-1/N-2) 7.99/7.82 (H-4), 7.73 (H-7), 7.45/7.37 (H-5), 7.33 (H-6), 5.80/5.79 (CH<sub>2</sub>-1'), 3.72 (CH<sub>2</sub>-2'), 3.17 (CH<sub>2</sub>-3'), 2.69 (-OH). (<sup>13</sup>C NMR, δ N-1/N-2) 145.8/144.3

(C-3a), 133.0 (C-7a), 127.9 (C-6), 124.3/126.9 (C-5), 119.8/118.2 (C-4), 110.0 (C-7), 65.7/66.3 (C-1'), 60.3 (C-3') 53.9 (C-2').

### Synthesis of 2-(bis((benzo[*d*] [1,2,3] triazol-1-yl) methylamino) ethyl acrylate (BMEA) and its polymerization to PBMEA

1g of compound 3 (3mmol) was dissolved in 6.5mL of acetone in a round bottom flask placed in an ice-water bath, with continuous stirring. Then, 0.50g (6mmol) of NaHCO<sub>3</sub> and 0.45mL (5.6mmol) of acryloyl chloride were added, the reaction was left to reach room temperature and followed by TLC. When starting material was consumed, salts were filtrated, and the solvent evaporated. The remaining solid was dissolved in 8 mL of methylisobutyl ketone and the flask purged twice with N<sub>2</sub>. Then, 0.13g of BPO (0.5mmol) were added, the system was purged again with N<sub>2</sub>, and then placed in a silicone bath at 75 °C for 48h. After that, a brownish-orange mass of PBMEA was obtained, which yield a light orange solid when treated with fresh acetone.

## Results and Discussion

In order to minimize the steric hindrance which could be exert the heterocycle on the polymerization reaction, we introduced a two-carbon spacer, using the benzotriazole capability to react with amines and formaldehyde [21]. applied synthetic scheme is shown in Figure 1. As expected in the characterization of compound 1 we have observed a mixture of *N*-1 and *N*-2 substitution (Figure 2), but the complexity of the spectra was too high for only two isomers. In the aromatic zone, even when displacements of all signals were in good agreement for *N*-1 and *N*-2 substituted 1,2,3-benzotriazoles [21], an unexpected signal at 7.76 δ appeared. The double triplet located at 7.76 δ suggested the existence of more deshielded H-7, which indicate a second *N*-1 substitution. A careful analysis of all aromatic signals and their coupling constants (when the spectrum allowed a first-order analysis) led us to conclude that there were four isomers in this mixture: two compounds with *N*-1 substitution (1a+1b) and two with *N*-2 substitution (1'a+1'b). The reaction of benzotriazole with aldehydes in presence of alcohols to give *N*-alkoxyalkyl benzotriazoles is described in literature [22], so we conclude that the reaction product includes aminoalkyl and alkoxyalkyl benzotriazoles as well. Proposed structures of compounds 1 and 1' are shown in Figure 3.

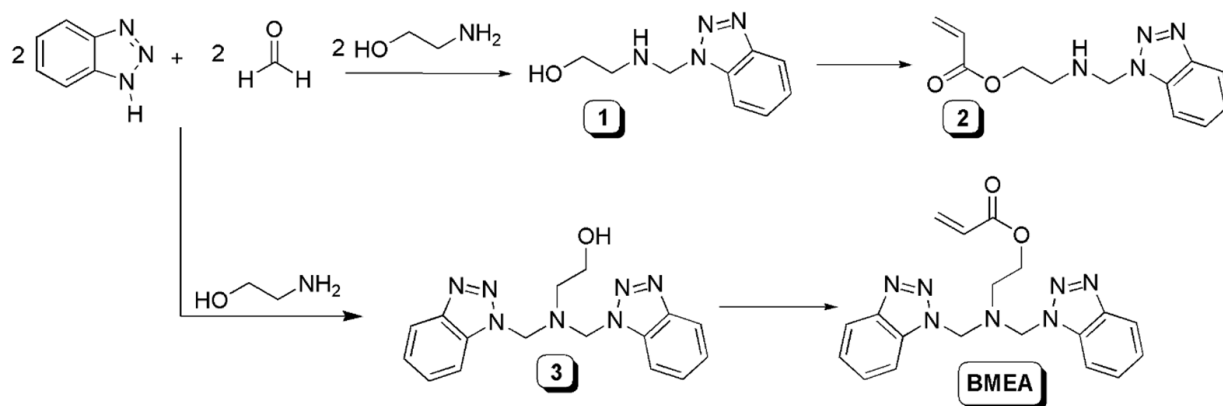
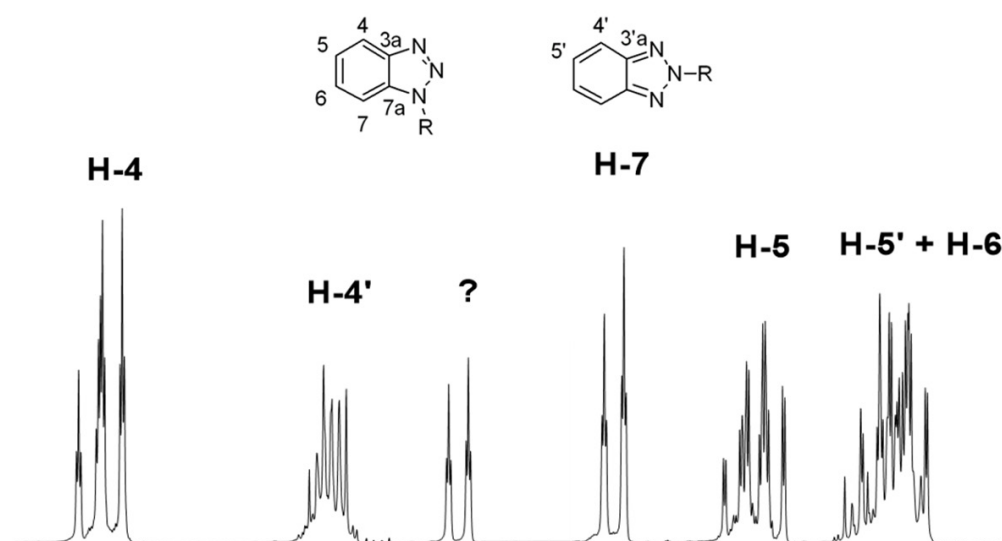
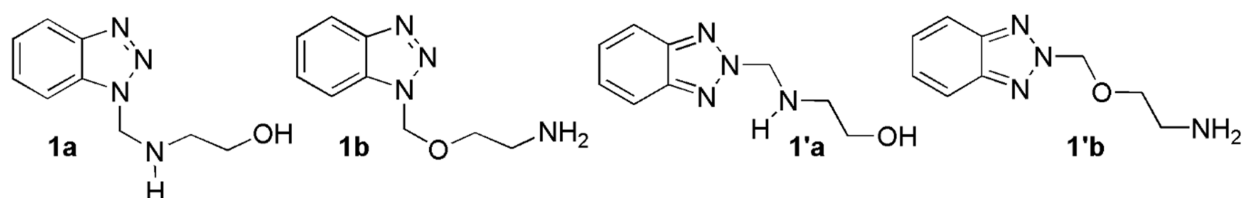


Figure 1: Proposed synthetic scheme for monomers.



**Figure 2:** Detail of the  $^1\text{H}$  NMR aromatic zone for mixture [1].

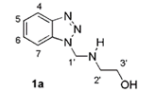


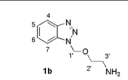
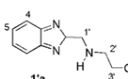
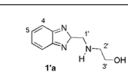
**Figure 3:** Structures for compounds 1a, 1b, 1'a & 1'b.

When comparing areas for both identified H-7 signals, we found a 7:4 ratio, with the smallest area corresponding to the signal with the highest  $\delta$ . Since oxygen usually exerts a greater deprotection effect than nitrogen, it could be concluded that the compound found in the highest proportion is compound 1a. So, the signal at 7.63  $\delta$  was assigned as H-7 from 1a isomer and signal at 7.76  $\delta$  as H-7 from 1b. From the comparison of areas corresponding to H-4 (1a+1b) and H-4' (1'a+1'b), we could estimate the existing molar relationship between *N*-1 isomers with respect to those alkylated at *N*-2. We found that the molar ratio between both substitutions is 13:10, which means an excess of 30% for the derivatives *N*-1 replacements. Given the signal superposition for both H-4' (1'a and 1'b), and signal of H-5' with the H-6, there is no possibility of estimate the ratio of 1'a vs 1'b. The rest of the  $^1\text{H}$  NMR signals were assigned using ACD-Lab and Mestre simulators, taking into account the relative areas (Table 1). Taking into account the complexity of the obtained mixture, and the possibility of a bis-acylation on 1a and 1'a (even its low probability by steric hindrance), we decided

not to proceed with the synthesis of the monomer 2 and work with a different molar ratio of reagents (benzotriazole: formaldehyde: ethanolamine, 2:2:1). As it was mentioned in literature [21], under these conditions, only *N*-1 substitution should be obtained. When NMR of compound 3 was performed it was clear that, even when the literature indicates that in this reaction only the *N*-1 alkylated derivative is obtained, we also found evidence of the presence of *N*-2 alkylation (3a+3b) (Figure 2). Based on the integral corresponding to H-4 and H-4' signals, we could estimate the molar proportion between *N*-1 and *N*-2 substituted rings, and it was around 5:1 relationship. Even when exist the possibility of formation of a third isomer with two *N*-2 substitution, we assume that this proportion was negligible, due to the low probability of *N*-2 substitution observed in this reaction. As for our final purposes the different substitution on the heterocycle was not critical, the monomer was synthesized starting of the mixture 3a+3b, and directly polymerized without monomer purification.

**Table 1:** Numbering and assignments of  $^1\text{H}$  NMR signals for compounds 1a, 1b, 1'a and 1'b.

Compound	H-4	H-5	H-6	H-7	CH <sub>2</sub> 1'	CH <sub>2</sub> 2'	CH <sub>2</sub> 3'	OH/NH
	8.06dt	7.50ddd	7.36m	7.63dt	5.60s			

	8.08dt	7.52ddd	7.39m	7.76dt	5.72s	3.62t 4.9	3.63t 4.9	
	7.87dd	7.40	-	-	5.60s	3.72t	2.73t	
	7.88dd	7.40	-	-	5.83s	3.81t	2.63t	3.27s

The PBMEA were obtained as a solid when treated with acetone and tends to soften in contact with air due to its great tendency to fix air moisture, even after it has been dried in a vacuum oven. As it was expected,  $^1\text{H}$  NMR recorded in DMSO- $d_6$  shows a big signal for water, as an intense and wide singlet, located at 3.76  $\delta$ . Even when water protons usually appear at 3.33  $\delta$  in DMSO- $d_6$ , this signal has not correlation with any carbon in HSQC spectrum. This behavior supports the assignment of 3.76  $\delta$  signal to water protons, so, the observed difference in displacement, although small, could be attributed to some type of interaction with the polymer. Between 7.33-8.11  $\delta$ , four complex signals are clearly visible, which are assignable to the aromatic ring protons, while a complex signal located around 4.80  $\delta$  is attributed to the methylene near the aromatic ring, because it does not present crossed peaks in the corresponding COSY spectrum. As expect for an atactic polymer,

the signals corresponding to the groups closest to the polymer chain are spread over a higher range of  $\delta$  than observed in 3 (3.1-3.8  $\delta$  vs. 2.2-5.0  $\delta$ ). In this range, triplet-shaped signals are clearly identifiable, corresponding to the spacer in different magnetic environments. The InfraRed spectrum (IR) of PBMEA offered few opportunities for analysis, since as it was seen in NMR, there is a large amount of water accompanying the material (Figure 4). For this reason, the most intense absorptions correspond to the O-H stretch ( $3430\text{cm}^{-1}$ ) and the bending movement ( $1640\text{cm}^{-1}$ ). However, there is evidence of the presence of aromatic rings ( $1587$ ,  $1460$  and  $1404\text{cm}^{-1}$ ) and of the carbonyl ester groups (as a shoulder at  $1693\text{cm}^{-1}$ ). There are minor absorptions at  $1074$ ,  $941$  and  $754\text{cm}^{-1}$ , the two first correspond to expansion and contraction ("breathing") of the triazole ring and the third corresponds to the out-of-plane aromatic C-H bending movements.

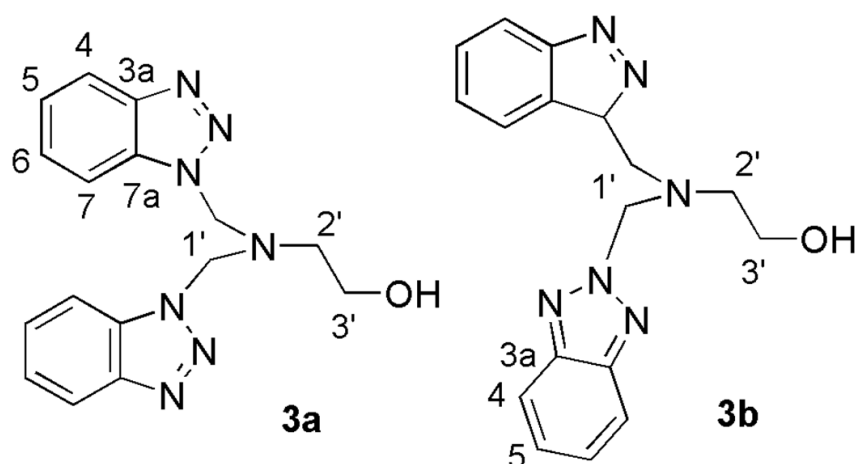


**Figure 4:** Molecular structure and numbering for compounds 3a and 3b.

When thermogravimetric analysis of PBMEA were performed, one of the notable things observed was the loss of a significant amount of water before 100  $^{\circ}\text{C}$ , which represents approximately 10% of the total (see Figure 5). Once the water has been removed, the material was stable up to 165  $^{\circ}\text{C}$ , where it began a decomposition process which shown a slight inflection at 225  $^{\circ}\text{C}$  (10.8%). After that, a second event of gradual decomposition began, which continues until about 400  $^{\circ}\text{C}$ , with a loss of more than 60% of the mass. At this point a final degradation process began, leaving a residual mass that represents 14% of the original mass. From

the amount of water losses from PMBEA and the corresponding molecular weights of water and the repeating unit, we were able to calculate a molar relationship between the water and the repeating unit and found a near 2:1 ratio. This quasi-stoichiometric value suggests some type of interaction between the repeating unit and the water. An optimization of the monomer structure was carried out using the HyperChem 8.0.7 program<sup>1</sup>. As it can be seen in Figure 6a, the aromatic rings are arranged in parallel in space, forming some kind of "clamp", which delimits a suitable place for the location of a hypothetical water molecule. Optimizations of the

<sup>1</sup>Calculations were made using semi empirical methods (AM1 force field) with Polak-Ribiere algorithm and RMS gradient of 0.01kcal/mol  $\text{\AA}$ .

monomer structure with two water molecules were also carried out and compared with the monomer. We found that two of these structures (Figures 6b & 6c) had an energy of around 450kcal/mol lesser than the monomer energy (Figure 6a). Taking into account

all these results, we can speculate that the macroscopic behavior of the PBMEA and its quasi-stoichiometric absorption of water comes from a direct interaction between the water and the pendant groups (heterocycles and spacers).

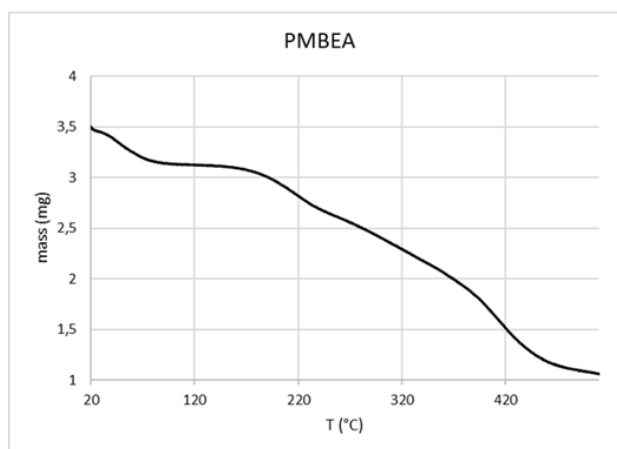


**Figure 5:** TGA for PBMEA.

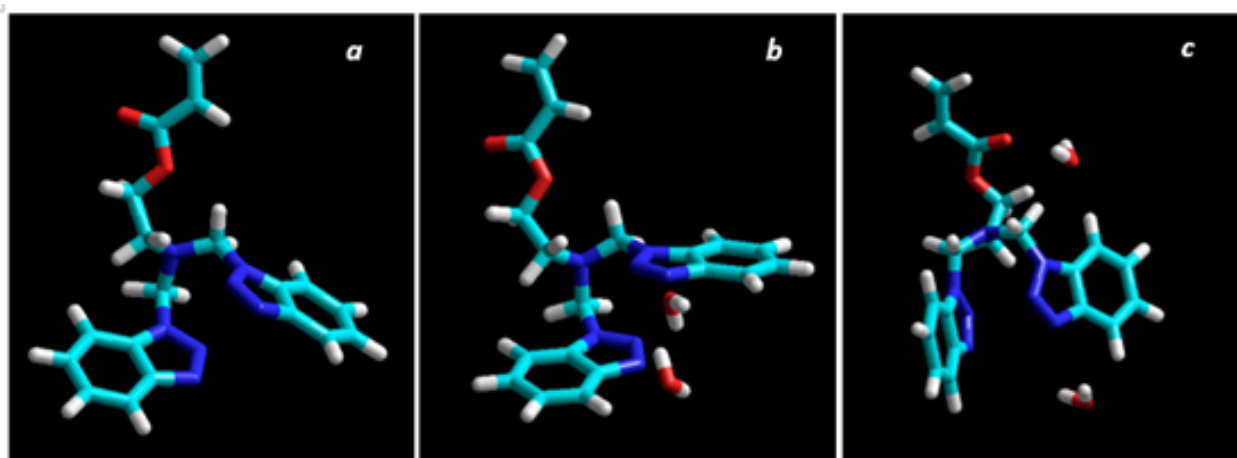


**Figure 6:** Minimum energy conformation for BMEA alone (a) for BMEA with two water molecules between Heterocycles (b) and for BMEA with one molecule between Heterocycles and another near to the Ethanolamine residue.

## Conclusion

In this work, we explored the reaction of 1,2,3-benzotriazole with ethanolamine and formaldehyde in two different reaction conditions. When a 1:1:1 molar relationship was used, we obtained a complex mixture of four regioisomers. On other hand, we were capable to achieve our main objective to obtain a material with pendant benzotriazole groups using a different mole ratio of reagents. In this case, two heterocycles for each monomeric unit were included. The analysis of its contribution to anticorrosive mixtures will be object of future studies, as planned. However, and as a result of the characterizations carried out, it became clear that PBMEA is a material that has other potential uses due to the possibility of including other ions or molecules than water between the two aromatic functions. Ion doping of this compound would allow to obtain materials with probable conduction capabilities.

Preliminary experiences that were carried out by putting this compound in contact with some heavy metal solutions indicated the retention capacity of the material, so alternative uses could be considered, such as purification of wastewater contaminated with heavy metals.

## Acknowledgement

The authors wish to thank to UBA for financial support to this research (UBACYT N° 20020190100339BA), to Teyupa S.A. for providing BPO and to Dr. María Inés Errea for her invaluable help.

## References

1. Nriagu JO (1994) Arsenic in the Environment: Cycling and Characterization. John Wiley & Sons, Inc: New York, USA, p. 448.
2. Sigman, Hazardous H (2000) Toxic Substance Policies. In: Portney PR, Stavins RN (Eds.), Public Policies for Environmental Protection, 2<sup>nd</sup>

- (edn), RFF Press Book, Washington, District of Columbia, USA, pp. 215-259.
3. Nava C, Worldwide C (1996) Overview of hazardous wastes. *Toxicol Ind Health* 12: 127-138.
  4. Kummer K (1992) The international regulation of transboundary traffic in hazardous wastes: The 1989 Basel Convention. *Int Comp Law Q41*: 530-562.
  5. UNEP (2006) Introduction to the Basel Convention: United Nations Environmental Program.
  6. (2010) Resource conservation and recovery act. Code of Federal Regulations, p. 261.
  7. Chandler AJ, Eighmy TT, Hjelmar, Kosson SE, Sawell J, Vehlow et al. (1997) Municipal solid waste incinerator residues, p. 67.
  8. Meadows DH, Meadows DL, Randers (1992) Beyond the limits: global collapse or a sustainable future. Earthscan Publications Ltd 68(4): 749-750.
  9. UNDP (1998) Human Development Report 1998. United Nations Development Program, Oxford University Press, UK.
  10. Moen AE (2008) Breaking Basel: The elements of the basal convention and its application to toxic ships. *Marine Policy* 32(6): 1053-1062.
  11. Ezeah, C, Roberts CL (2012) Analysis of barriers and success factors affecting the adoption of sustainable municipal solid waste management in Nigeria. *Journal of environmental management* 103: 9-14.
  12. Scheinberg A (2011) Value-added: Modes of sustainable recycling in the modernization of waste management systems.
  13. Mu Y (2006) Developing a suitability index for residential land use: A case study in dianchi drainage area (master's thesis, university of Waterloo).
  14. Shalabi AMA, Mansor SB, Ahmed (2006) GIS-based multicriteria approaches to housing site suitability assessment. In XXIII FIG Congress, Shaping the Change, Munich, Germany, pp. 8-13.
  15. Lyon JG (1987) Use maps, aerial photographs, and other remote sensor data for practical evaluations of hazardous waste sites *Photogramm Eng Remote Sensing* 53: 515-519.
  16. Getz TJ, Randolph JC, Echelberger (1983) Environmental application of aerial reconnaissance to search for open dumps *Environ Manage* 7: 553-562.
  17. Herman JD, Waites JE, Ponitz (1994) A temporal and spatial resolution remote sensing study of a Michigan Superfund site *Photogram Eng Remote Sensing* 60: 1007-1017.
  18. Ottavianelli G, Hobbs S, Smith (2005) Assessment of hyperspectral and SAR Remote sensing for solid waste landfill management. Proceedings of the 3<sup>rd</sup> ESA CHRIS/Proba Workshop, Frascati, Italy, p. 8.
  19. Donald MGT, Brown AL (1984) The land suitability approach to strategic land-use planning in urban fringe areas. *Landscape Planning* 11(2): 125-150.
  20. Chopra A (2020) Paradigm shift and challenges in IoT security. IOP Publishing, UK.